SLAC-PUB-14257
September 2010

# HIGHER ORDER MODE HEATING ANALYSIS FOR THE ILC SUPERCONDUCTING LINACS*

K.L.F. Bane, C. Nantista, C. Adolphsen,
SLAC National Accelerator Laboratory, Stanford, CA 94309, USA

*Presented at the 25th International Linear Accelerator Conference (LINAC10), Tsukuba, Japan, 12–17 September 2010*

*Work supported by Department of Energy contract DE–AC02–76SF00515.

# HIGHER ORDER MODE HEATING ANALYSIS FOR THE ILC SUPERCONDUCTING LINACS *

K. Bane, C. Nantista, C. Adolphsen, SLAC, Stanford, CA 94309, USA

## INTRODUCTION

The superconducting cavities and interconnects in the 11 km long linacs of the International Linear Collider (ILC) are designed to operate at 2K, where cooling costs are very expensive. It is thus important to minimize cryogenic heat loads. In addition to an unavoidable static load and the dynamic load of the fundamental 1.3 GHz accelerating rf, a further heat source is presented by the higher order mode (HOM) power deposited by the beam. Such modes will be damped by specially designed HOM couplers attached to the cavities (for trapped modes), and by ceramic dampers at 70K that are located between the eight or nine cavity cryomodules (for propagating modes).

Brute force calculation of the higher frequency modes excited in a string of cryomodules is limited by computing capacity (see, *e.g.* [1]). M. Liepe has calculated $\sim$ 400 longitudinal TM modes in 3 superconducting cavities plus absorbers, up to 8 GHz [2]. Jöstingmeier, *et al.*, have used a ray tracing calculation to find the effect at higher frequencies, specifically in the range of tens of GHz and above [3]. In this report we present a scattering matrix approach, which we apply to an rf unit comprising 26 cavities and 3 absorbers. We perform calculations at sample frequencies (up to 20 GHz) to predict the effectiveness of the ceramic dampers in limiting HOM heat deposition at 2K.

## S-MATRIX FORMULATION

For the purposes of this report we consider an ILC linac rf unit to comprise a finite string of beamline objects that, at a given frequency, can be described by the S-matrix formalism. A simple example is sketched in Fig. 1; we show two objects in a string, with each object coupling through four ports (the horizontal lines). Here, for a particular frequency $f$, $\mathbf{S}_{n-1}$ is the $4\times 4$ S-matrix that describes the relative field voltage transmitted and reflected between physical junctions $n-1$ and $n$. The ports represent coupling through a beam pipe monopole mode; the fact that there are two ports on each side of the objects in the figure means that, in this example, there are two monopole modes above cut-off at frequency $f$.

In the case of only one beam pipe mode, the voltage of the right-going and left-going waves at junction $n$, denoted by $r_n$ and $l_n$, respectively, is related to that in neighboring junctions by

$$\begin{aligned} r_n &= (S_{n-1})_{21} r_{n-1} + (S_{n-1})_{22} l_n \\ l_n &= (S_n)_{11} r_n + (S_n)_{12} l_{n+1} \,. \end{aligned} \tag{1}$$

Note that the S-matrix is symmetric, with $S_{12} = S_{21}$.

* Work supported by the U.S. Department of Energy under contract DE-AC02-76SF00515.

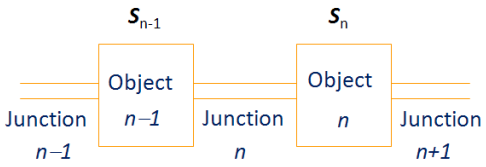


Figure 1: Schematic of a simple string of beamline objects coupling through two beam pipe modes.

With $M$ modes the equations concerning physical junctions $n$ and $n+1$ can be written as

$$\begin{aligned} &(l_{n,1}, l_{n,2}, ..., l_{n,M}, r_{n+1,1}, r_{n+1,2}, ..., r_{n+1,M})^T = \\ &\quad \mathbf{S}(r_{n,1}, r_{n,2}, ..., r_{n,M}, l_{n+1,1}, l_{n+1,2}, ..., l_{n+1,M})^T \end{aligned} \tag{2}$$

where $l$ and $r$ now have two indices, junction number and mode number; $^T$ means to take the transpose; $\mathbf{S}$ is a $2M \times 2M$ scattering matrix between junctions $n$ and $n+1$ (the ordering of indices is the same as for the vectors in Eq. 2).

At the ends of the basic rf unit, comprising three cryomudules, we apply periodic boundary conditions, *i.e.* for all modes $m$ we let

$$r_{1,m} = r_{N+1,m} e^{2\pi i f L/c} \,, \quad l_{N+1,m} = l_{1,m} e^{-2\pi i f L/c} \,, \tag{3}$$

where $L$ is the rf unit length and $c$ is speed of light. The conditions reflect the linac periodicity and the fact that the HOM's are driven by a speed of light beam (moving to the right).

In our calculations, to simulate wakefield excitation by the beam, we include a driving term moving rightward in mode 1,

$$d_{n',1} = e^{-2\pi i f z_{n'}/c} \,, \tag{4}$$

with $n'$ limited to the downstream junctions of the cavities and $z_{n'}$ the location of this junction ($z=0$ at the beginning of the rf unit); all other $d_{n,m}$ are set to zero. In reality the beam excites the different beam-pipe modes at specific amplitudes. We are only interested in the relative power deposition in the absorbers *vs.* the other objects (so we can use an arbitrary scale factor) and we are counting on mode conversion to make us insensitive to the relative excition of the different modes (a point that we test below).

We can write Eqs. 2-4 as the matrix equation

$$\mathbf{A}\mathbf{y} = \mathbf{d} \,, \tag{5}$$

which can be solved for $\mathbf{y}$, which contains the right and left going voltages in all the junctions, in all the modes. With $N$ objects and $M$ modes the order of the matrix $\mathbf{A}$, and the number of unknowns, is $2M(N+1)$. Note that, because of the normalization of the driving term, our solution will only have information about the relative value of the voltage excited in the different junctions.

The element $y_i$ gives the voltage in one direction, in one of the junctions, in one of the modes, and $|y_i|^2$ gives the power (both in arbitrary units). The power deposited in an object that has no driving term (is not a cavity) is $p = \sum_m (|y_{in}|^2 - |y_{out}|^2)$, where the sum is over the $m$ modes, and $|y_{in}|^2$ ($|y_{out}|^2$) is the power moving toward (away from) the object. In general the power deposited in object $n$ (between physical junctions $n$ and $n+1$) is

$$p_n = \sum_m (|r_{n,m}|^2 + |l_{n+1,m}|^2 - |l_{n,m}|^2 - |r_{n+1,m}|^2) + |r_{n+1,1}|^2 - |r_{n+1,1} - d_{n+1,1}|^2 \ , \quad (6)$$

since our drive moves to the right in mode 1.

## THE BASIC RF UNIT

The collection of beamline objects in a basic rf unit of the ILC linacs—which can be divided into three equal-length pieces—is sketched in Fig. 2. In this unit there are 26 rf cavities (cav), three absorbers (abs), and one drift or spacer (drift) at the location of a quadrupole magnet. Also to be included in our calculations, but not shown, are bellows connecting all the objects together. The nominal total length $L = 37.956$ m. All objects are modeled as cylindrically symmetric and have beam pipes of radius 39 mm.

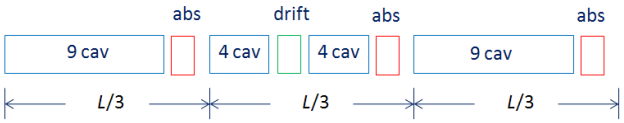


Figure 2: Arrangement of beamline objects in an ILC basic rf unit. Also included in our calculations, but not shown, are bellows connecting all objects together.

HFSS scattering matrix calculations [4] were performed for the different types of objects at frequencies $f = 4$, 8, 12, 16, 20 GHz (see Fig. 3). Note that the first 6 $\mathrm{TM}_{0,m}$ beam pipe cut-off frequencies are 2.94, 6.76, 10.59, 14.44, 18.28, 22.12 GHz; thus we see that there are $i$ modes in the calculation for the $i^{\mathrm{th}}$ sample frequency, as many as 5 modes for $f = 20$ GHz. In the HFSS calculations, except for the case of the bellows and absorbers, the beamline objects were modeled as being perfectly conducting. We consider the beam pipes for all objects to be Cu plated at 2K (conductivity $\sigma = 10^{10}\ \Omega^{-1}\mathrm{m}^{-1}$); so the S-matrices obtained by HFSS were modified to include pipe losses:

$$S_{ij} \to C_i S_{ij} C_j \ , \quad \text{where} \quad C_i = e^{-\bar{\alpha}_i l_0} \ , \qquad (7)$$

with $l_0$ the length of each beam pipe. The parameters: $\bar{\boldsymbol{\alpha}} = (\alpha_1, ..., \alpha_M, \alpha_1, ..., \alpha_M)^T$; $\alpha_i = 2\pi f R_s/(caZ_0\beta_i)$, $\beta_i = [(2\pi f/c)^2 - (j_{0i}/a)^2]^{1/2}$, $R_s = (\pi Z_0 f/\sigma c)^{1/2}$; where $a$ is beam pipe radius, $Z_0 = 377\ \Omega$ and $j_{0i}$ is the $i^{\mathrm{th}}$ zero of Bessel function $J_0$.

The objects, their beam pipe lengths, and their total lengths are: (9-cell) rf cavity, 264 mm, 1.216 m; drift tube, 1.216 m, 1.216 m; absorber 548 mm, 608 mm; bellows, 51 mm, 110 mm. The absorbers (at 70K) are estimated to have $\tan\delta = 0.23 - 7.5 \times 10^{-3} f$ [GHz][5]; in our calculations the pipes of the absorbers are separated (since they are at 2K) and they become their own beamline objects. The bellows are entirely Cu plated, at 2K. The total number of objects in a basic rf unit, and thus our calculations, is $N = 66$. At $f = 20$ GHz, where there are $M = 5$ modes, the order of the matrix equation that needs to be solved is $2M(N+1) = 670$.

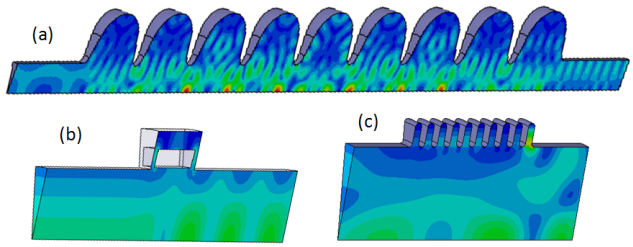


Figure 3: Output of sample HFSS calculations on 10° wedges of: (a) an ILC cavity, (b) an absorber, (c) a bellows. In all cases the beam pipe radius is 39 mm.

As an indicator of effectiveness of the absorbers we will use

$$p_{2K}/p_{tot} = 1 - p_{abs}/p_{tot} \ ,$$

with $p_{2K}$ and $p_{abs}$, respectively, the power deposited at 2K (into the Cu) and at 70K (into the absorbers).

## RESULTS

We perform calculations of $p_{2K}/p_{tot}$ at the five sample frequencies (see Table 1, the column labeled nom(inal)). At $f = 4$ GHz, 17.2% of the power is deposited at 2K; at the other frequencies, less than 1% is. In Fig. 4 we plot, for $f = 4$ GHz, the absolute value of the field $|y|$; we note that the loss is large because the absorbers are at nodes.

Table 1: Nominal result and statistics for $p_{2K}/p_{tot}$ when varying cavity beam pipe length randomly, with $\sigma_z = 2$ mm ( in [%] ).

| f [GHz] | nom | ave | rms | 0.9 quant |
|---|---|---|---|---|
| 4 | 17.2 | 15.3 | 5.2 | 21.7 |
| 8 | 0.3 | 0.4 | 0.1 | 0.5 |
| 12 | 0.4 | 0.4 | 0.1 | 0.6 |
| 16 | 0.4 | 6.2 | 12.7 | 18.0 |
| 20 | 0.7 | 6.4 | 13.6 | 15.4 |

To study the sensitivity of the results to the exact geometry, we add a random length of rms $\sigma = 2$ mm to the cavity pipes, and repeat the calculation. Changing the beam pipe lengths of a cavity by $\Delta z/2$ (at each end) will change its S-matrix according to Eq. 7, except with $C_i = e^{-(\bar{\alpha}_i - i\bar{\beta}_i)\Delta z/2}$, where $\bar{\boldsymbol{\beta}} = (\beta_1, ..., \beta_M, \beta_1, ..., \beta_M)^T$. In

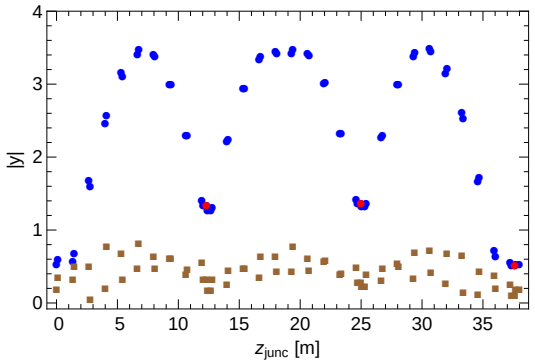


Figure 4: For $f = 4$ GHz: the quantity $|y|$ for right going waves (blue) and left going waves (brown); $|r_{n,1}|$ for absorbers is shown in red. For this case $p_{2K}/p_{tot} = 0.17$.

Table 1, for 800 samples at each frequency, we give the average, rms, and 0.9 quantile of the resulting $p_{2K}/p_{tot}$. We see that at 16 and 20 GHz the result is sensitive to beam pipe length, and the average loss at 2K becomes $\sim 6\%$.

Ideally to find the power deposition in the frequency gaps in our calculations, we should perform more HFSS calculations and repeat our process. However, instead, for our five frequencies, we perform calculations for the rf unit with systematically lengthened cavity beam pipes, and take the statistics of these results as indicators of absorber efficiency over the frequency intervals. For each frequency we calculate for 2000 steps, with a maximum total length added per cavity of $(\Delta z)_{max} = 2\pi/\beta_M$ (where $M$ is the highest beam pipe mode number). Results of $p_{2K}/p_{tot}$ *vs.* $\Delta z$, for the case of $f = 16$ GHz, are shown in Fig. 5.

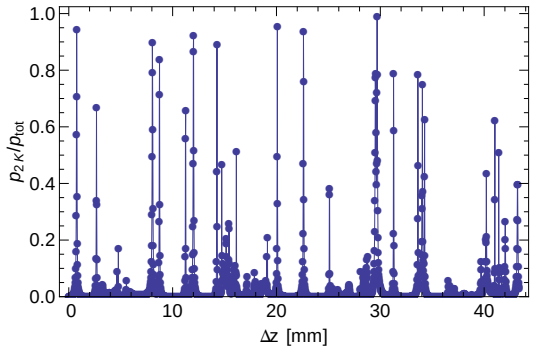


Figure 5: For $f = 16$ GHz: $p_{2K}/p_{tot}$ *vs.* systematic change in cavity beam pipe length $\Delta z$.

In the plot we see some highly peaked values among mostly smaller results. Some of the higher points correspond to wave patterns that have nodes in the region of the absorbers (as was seen in Fig. 4). But many consist of a very localized pattern that is near zero at the absorbers. In Fig. 6 we show one such example for $f = 16$ GHz. We show only the $m = 1$ right and left going wave pattern, for clarity—the higher mode patterns look similar.

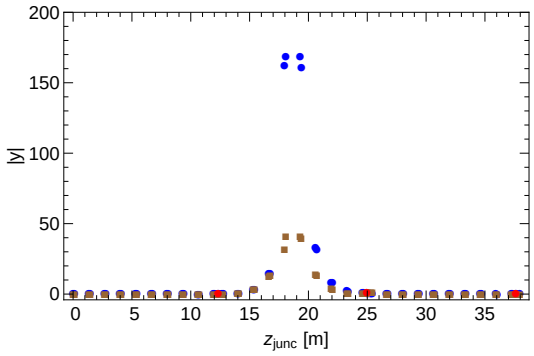


Figure 6: For $f = 16$ GHz and $\Delta z = 0.8$ mm: $|y|$ for right (blue) and left (brown) going waves in the first mode ($m = 1$); $|r_{n,1}|$ for absorbers is in red; $p_{2K}/p_{tot} = 0.95$.

The average, rms, and 0.9 quantile of the systematically lengthened beam pipe results are given in Table 2. We see that the expectation value of $p_{2K}/p_{tot}$ varies from 1.4–8.0%. Finally, for $f = 16$ GHz, we repeated the calculation but allowed the driving terms to be in a higher beam pipe mode (see Table 3). We see that the statistical results are relatively insensitive ($\sim 25\%$) to which mode is driven.

Table 2: Statistics for $p_{2K}/p_{tot}$ when varying cavity beam pipe length systematically ( in [%] ).

| f [GHz] | ave | rms | 0.9 quant |
|---|---|---|---|
| 4 | 8.0 | 7.0 | 15.7 |
| 8 | 2.8 | 6.6 | 5.9 |
| 12 | 1.4 | 3.8 | 2.2 |
| 16 | 4.0 | 11.8 | 7.0 |
| 20 | 5.9 | 10.5 | 13.5 |

Table 3: For $f = 16$ GHz, when the beam driving mode is $m$: Statistics for $p_{2K}/p_{tot}$ when varying cavity beam pipe length systematically ( in [%] ).

| m | average | rms | 0.9 quant |
|---|---|---|---|
| 1 | 4.0 | 11.8 | 7.0 |
| 2 | 3.2 | 9.1 | 5.2 |
| 3 | 4.1 | 11.1 | 8.1 |
| 4 | 3.4 | 9.4 | 6.5 |

## REFERENCES

[1] M. Dohlus, see http://www.desy.de/fel-beam/data/talks/talks/dohlus_-_cryo_calc_20071112.pdf.

[2] M. Liepe, Proc. of SRF03, Travemuende, 2003.

[3] A. Jöstingmeier et al, TESLA 2000-11, DESY, 2000.

[4] HFSS, Ansys, Inc.

[5] Mildner et al, Proc. of SRF05, Cornell, 2005.